Talanta 117 (2013) 511–517

Contents lists available at ScienceDirect

Talanta

journal homepage: www.elsevier.com/locate/talanta

Synthesis and characterization of poly[1-(N,N-*bis*-carboxymethyl) amino-3-allylglycerol-*co*-dimethylacrylamide] grafted to magnetic nano-particles for extraction and determination of letrozole in biological and pharmaceutical samples

Homayon Ahmad Panahi [a,*], Elham Reza Soltani [a], Elham Moniri [b], Atefeh Tamadon [a]

[a] Department of Chemistry, Central Tehran Branch, Islamic Azad University, Tehran, Iran
[b] Department of Chemistry, Varamin (Pishva) Branch, Islamic Azad University, Varamin, Iran

ARTICLE INFO

Article history:
Received 9 May 2013
Received in revised form
6 September 2013
Accepted 10 September 2013
Available online 3 October 2013

Keywords:
Letrozole
Solid phase extraction
Pharmaceutical samples
Human biological fluids
Breast cancer
Enteric drug delivery

ABSTRACT

In this paper, a new method is reported for the surface grafting of poly[1-(N,N-bis-carboxymethyl) amino-3-allylglycerol-co-dimethylacrylamide] onto magnetic nano-particles modified by 3-mercaptopropyltrimethoxysilane. The grafted nano-sorbent was characterized by Fourier transform infrared spectroscopy, elemental analysis, thermogravimetric analysis, and scanning electron microscopy. Agglomerated nano-particles with multi-pores were used for extraction and determination of trace letrozole in human biological fluids and pharmaceutical samples. The profile of the letrozole uptake by the magnetic nano-sorbent reflected good accessibility of the active sites in the grafted polymer. Scatchard analysis revealed that the sorption capacity of the functionalized nano-sorbent was 6.27 μmol g^{-1} at an optimum pH of 4. The equilibrium adsorption data of letrozole by grafted magnetic nano-sorbent were analyzed by Langmuir, Freundlich, Temkin and Redlich–Peterson models. Conformation of the experimental data in the Langmuir isotherm model indicated the homogeneous binding site of functional polymer-grafted magnetic nano-sorbent surface. Nearly 89% of letrozole was released in simulated gastric fluid, pH 1.2, in 2 h and 79% in simulated intestinal fluid, pH 7.4, in 30 h. These results show the utility of the letrozole loaded- polymer grafted magnetite nano-particles for enteric drug delivery.

1. Introduction

Letrozole, a third-generation aromatase inhibitor, is one of the most common drugs for patients with malignant breast cancer [1–9]. This drug is many times more specific and potent than aminoglutethimide, tamoxifen, and other drugs used for this type of cancer. Breast cancer is the most common type of cancer, especially in women, and, unfortunately, its incidence is increasing each year [10]. It is responsible for nearly 20% of all cancer deaths in women. The lifetime risk of developing this type of cancer is one in ten. Patients who suffer from this cancer most commonly use tamoxifen to minimize the recurrence risk. There is good evidence that aromatase inhibitors are powerful new alternative drugs and are more active than tamoxifen as neoadjuvant therapy in the treatment of breast cancer.

Developments in the control of nano-particles' shape and size continue, because many of their properties are size-dependent. Recently, nano-scaled magnetic particles have received more attention because of their potential applications in many biological and industrial fields, such as targeted drug delivery [11–15], especially in cancer therapy. Nano-magnetite are easily obtained through various chemical synthetic techniques, including co-precipitation, hydrothermal techniques, sol–gel methods, laser pyrolysis methods, the reverse micelle techniques, and ultra-sound irradiation. Surface modification by grafting organic polymer chains to solid supports is a significant technique for the creation of a sorbent with a great surface and usable for specific drug sorption. Polymer grafting is a method of attaching polymers to active groups on solid support surfaces [16]. Grafted polymers offer unique opportunities to have a sorbent with specific sorption and/ or high capacity [17–19].

In this research, magnetite nanoparticles were synthesized by the co-precipitation method, and the free-radical graft co-polymerization of 1-(N,N-*bis*-carboxymethyl)amino-3-allylglycerol, a functional monomer, and N, N-dimethylacrylamide onto magnetic nano-particle surface modified with (3-mercaptopropyl)trimethoxy silane is reported. The purpose of the present study is to indicate the feasibility of using this grafted magnetic nano-particle as a solid

* Corresponding author. Tel./fax: +98 21 44164539.
E-mail address: h.ahmadpanahi@iauctb.ac.ir (H. Ahmad Panahi).

0039-9140/$ - see front matter © 2013 Elsevier B.V. All rights reserved.
http://dx.doi.org/10.1016/j.talanta.2013.09.015

sorbent for the extraction of letrozole from biological fluids and pharmaceutical samples. The polymer-grafted magnetic nano-sorbent was also used for effective enteric drug delivery. Moreover, the field of drug delivery has been faced with the task of providing sustained release of a therapeutic agent over a prolonged period of time [20–23]. The synthesized nano-sorbent released about 80% of letrozole in conditions of the human body after 30 h.

2. Experimental

2.1. Instruments

Infrared spectra were recorded on a Jasco Fourier transform infrared spectrometer (FT-IR-410, Jasco Inc., Easton, Maryland, USA). Elemental analysis was carried out on a Thermo-Finnigan (Milan, Italy) model Flash EA elemental analyzer. Thermogravimetric analysis was carried out using a TGA-50H (Shimadzu Corporation, Kyoto, Japan). The scanning electron microscopy (SEM) micrographs were obtained on a SEM-PHILIPS XL30 scanning electron microscopy.

2.2. Reagents and solutions

N, N-Dimethylacrylamide, and 3-mercaptopropyltrimethoxysilane were obtained from Steinheim, Germany. 2,2′-Azobis (2-methylpropionitrile) was purchased from Acros (New Jersey, USA). Allyl glycidyl ether was purchased from Fluka Chemica (Buchs, Switzerland). Anhydrous 1,4-Dioxane, iminodiacetic acid, acetic acid (AcOH), trifluoroacetic acid (TFA), ethanol, methanol, and all the inorganic acid and salt were products of Merck (Darmstadt, Germany).

All reagents were of analytical grade and used without any further purification.

The stock solution (500 mg L^{-1}) of letrozole was prepared in methanol. To adjust the pH of the solution, either an acetate buffer or a phosphate buffer was used wherever suitable.

2.3. Synthesis of functional polymer-grafted magnetic nano-particles (FPG-MNP)

2.3.1. Preparation of magnetic nano-particles

Magnetic nano-particles were synthesized through the co-precipitation technique [24]. The ammonia solution was added to 100 mL of solution containing $FeCl_3 \cdot 6H_2O$ (2.31 g) and $FeCl_2 \cdot 4H_2O$ (3.97 g) under conditions of a nitrogen atmosphere and vigorous mechanical stirring. The solution was left to be stirred for 2 h more at 85 °C. The resulting magnetic nano-inorganic oxide particles were separated magnetically, then washed with distilled water and ethanol and dried under vacuum in a desiccator over dry calcium chloride.

2.4. Preparation of the functional monomer 1-(N,N-bis-carboxymethyl)amino-3-allylglycerol

Details of the synthesis and characterization of the 1-(N,N-bis-carboxymethyl)amino-3-allylglycerol was mentioned in the previous work [25]. At first, the iminodiacetic acid was neutralized with a potassium hydroxide solution.The dipotassium salt of the iminodiacetic acid solution was slowly added to the allyl glycidyl ether at a 1:1 M ratio. The mixture was kept at 65 °C for 1 h under vigorous stirring conditions, so the oil–water mixture became a transparent water phase. The yellowish liquid monomer was purified by being poured into acetone and dissolved in water repeatedly. The resulting product was confirmed as the functional monomer by FT-IR, ^{1}H-NMR and ^{13}C-NMR.

2.5. Polymer grafting

Our plan for graft polymerization onto magnetic nano-particles is free-radical polymerization. Free-radical graft polymerization onto inorganic oxide support requires modification of the surface by bonding reactive functional sites such as organosilanes. At first, magnetic nano-particles should be modified with 3-mercapto-propyltrimethoxysilane, and then a functional polymer should be grafted to the modified magnetic nano-particles.

2.6. Modification of magnetic nano-particles with 3-mercaptopropyltrimethoxysilane

Magnetic nano-particles (3 g) were silylated by a solution of 5% of 3-mercaptopropyltrimethoxysilane in anhydrous 1, 4-dioxane. The silyation reaction was performed in the boiling solution for 48 h. The modified magnetic nano-particles were then washed two times with 1, 4-dioxane and dried under vacuum in a desiccator over dry calcium chloride.

2.7. Polymerization

The free radical graft copolymerization of 1-(N,N-bis-carboxymethyl)amino-3-allylglycerol-co-dimethylacrylamide onto modified magnetic nano-particles was carried out in a temperature-controlled reactor under conditions of powerful stirring and a nitrogen atmosphere. The modified magnetic nano-particles were placed into the degassed polymerization mixture (20 mL ethanol as solvent, 20 mL 1-(N,N-bis-carboxymethyl)amino-3-allylglycerol as functional monomer, 2 mL N, N-dimethylacrylamide, and 0.1 g 2,2′-azobis (2-methylpropionitrile) as initiator) for 7 h at 70 °C. The functional polymer-grafted magnetic nano-particles (FPG-MNP) were immediately separated from the solution with a magnet and washed with 50 mL of ethanol to remove any homopolymer that may have adsorbed. Then they were dried under vacuum in a desiccator over dry calcium chloride. The methodology used to synthesize FPG-MNP is summarized in Fig. 1. The FPG-MNP was characterized by FT-IR, elemental analysis, TGA and SEM.

2.8. HPLC System

Chromatographic separations were carried out on an Agilent HPLC, 1200 series, equipped with a UV/vis detector. Separations were carried out on a Zorbax Extend C18 column (15 cm − 4.6 mm, with 3 mm particle size) from the Agilent Company (Wilmington, DE, USA). The mixture of acetonitrile and phosphate buffer (pH=6.8) (56:44 v/v), at a flow rate of 1 mL min^{-1}, was used as a mobile phase in isocratic elution mode. The injection volume was 20 μL for all samples, and the detection was performed at a wavelength of 242 nm.

2.9. Batch method of letrozole adsorption/desorption

A set of solutions (1 mL) containing 1–60 μg mL^{-1} of letrozole was taken in a micro-test tube, and their pH levels were adjusted to 4 with a buffer solution. FPG-MNP (0.01 g) was added to each solution, and the mixture was vortexed for 2 min. The FPG-MNP was separated magnetically, and the sorbed letrozole was eluted with methanol/AA/ TFA. The concentration of letrozole in the eluate was determined by HPLC.

2.10. Isotherm studies

Isotherm studies were performed by adding 0.05 g of FPG-MNP to a series of test tubes filled with 10 mL diluted solutions of

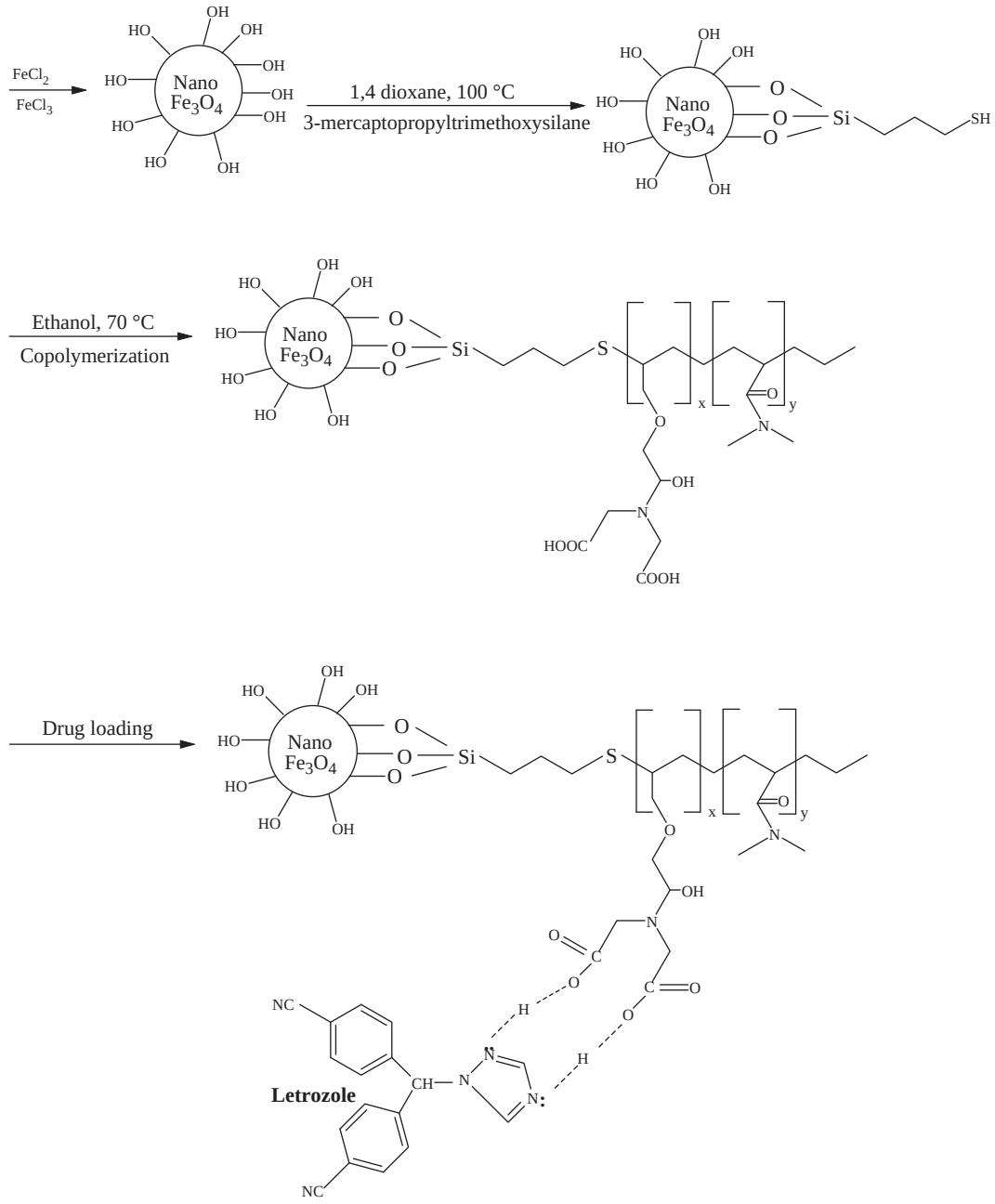

Fig. 1. Schematic presentation of synthesis and grafting process of FPG-MNP.

letrozole (1–60 μg mL^{-1}) in acetate buffer, pH 4. The tubes were then sealed and vortexed at 20 °C for 20 min. The amount of letrozole at equilibrium q_e (mg g^{-1}) on FPG-MNP was calculated using the following equation:

$$q_e = (C_0 - C_e)V/W \quad (1)$$

where C_0 and C_e (mg L^{-1}) are initial and equilibrium concentrations of the letrozole, respectively, V (L) is the volume of the solution, and W (g) is the mass of the FPG-MNP.

2.11. In vitro drug release

The release profiles of letrozole from FPG-MNP were determined in simulated gastric fluid (pH 1.2) and simulated intestinal fluid (pH 7.4). The letrozole-loaded FPG-MNP was put into beakers with shaking (30 rpm) and without shaking at 37 °C. At scheduled time intervals, samples were taken, and the letrozole content of each sample was determined by HPLC.

3. Results and discussion

3.1. Characterization

FT-IR spectrum revealed that the copolymer was grafted to the magnetic nano-particles as shown in Fig. 1. The peaks at 579.21 cm^{-1} and 3391.41 cm^{-1} were related to Fe–O stretching band and O–H stretching, respectively. Table 1 shows additional peaks in 3-mercaptopropyltrimethoxysilane-magnetic nano-particles, which indicates the existence of S–H groups after modification. The peaks of C–O, carbonyl, and hydroxyl groups in FPG-MNP confirmed that grafting was done successfully (see Table 1). The data used for elemental analysis are listed in Table 1. Sulfur and

Table 1
Fourier transformation-infrared and elemental analysis information.

Fourier transformation-infrared				
Magnetic nano-particles	579.21 cm^{-1} Fe–O stretching	3391.41 cm^{-1} O–H stretching		
3-mercaptopropyltrimethoxysilane- Magnetic nano-particles	2919.34 cm^{-1} C–H stretching	2309.39 cm^{-1} S–H stretching		
FPG-MNP	1068 cm^{-1} C–O stretching	1627 cm^{-1} C=O stretching	3401 cm^{-1} OH stretching	
Elemental analysis				
	C (%)	N (%)	H (%)	S (%)
Magnetic nano-particles	0.01	0.05	0.53	0.02
3-mercaptopropyltrimethoxysilane- Magnetic nano-particles	2.93	0.03	0.62	2.20
FPG-MNP	4.34	0.42	0.93	1.82

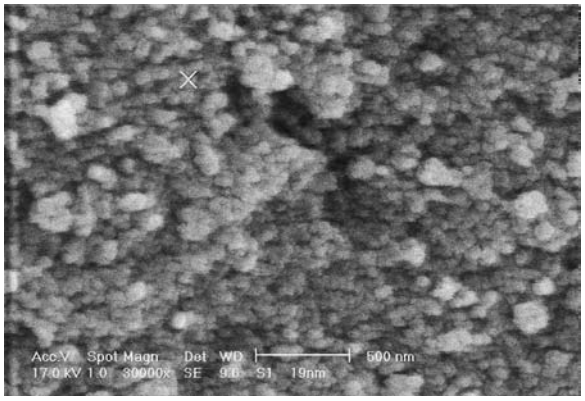

Fig. 2. SEM image of FPG-MNP.

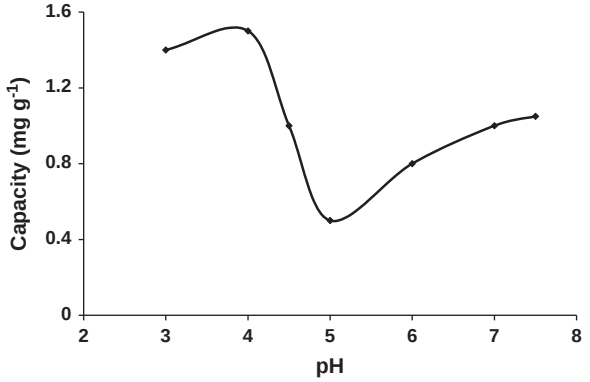

Fig. 3. Effect of pH on sorption of letrozole onto FPG-MNP.

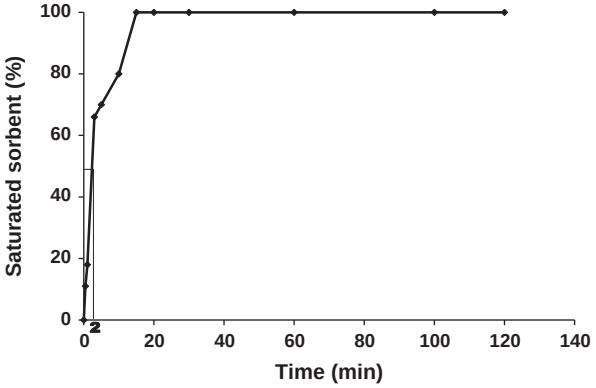

Fig. 4. Kinetics of letrozole sorption on FPG-MNP.

carbon percentages in 3-mercaptopropyltrimethoxysilane-magnetic nano-particles as well as the nitrogen and carbon percentages in FPG-MNP confirmed the structure of FPG-MNP as shown in Fig. 1. The thermal behavior of the magnetic nano-particles was studied by thermogravimetric analysis and compared with FPG-MNP. The thermogravimetry of magnetic nano-particles showed a 4.4% weight loss up to 600 °C; due to the removal of adsorbed water and water molecules from the structure of the particles; whereas FPG-MNP indicated an 8.9% weight loss up to 600 °C therefore 4.5% of the weight loss was due to the decomposition of the polymeric matrix on the magnetic nano-particles. The morphology and particle size of FPG-MNP were analyzed using SEM. Fig. 2 indicates the spherical agglomerated nano-particles with an average diameter of less than 100 nm. The SEM image also indicates that the surface of agglomerated FPG-MNP is not smooth.

3.2. Optimization of parameters

The degree of letrozole sorption at different pH values (3–8) was investigated using the batch method. The experimental results given in Fig. 3 show that best sorption was carried out at pH 4. The higher extraction of letrozole at a lower pH may be due to the enhanced protonation of carboxylic acidic groups on the surface of FPG-MNP and the subsequent increase of hydrogen bonding with nitrogen atoms in letrozole. The protonation decreases with increasing pH, so the electrostatic repulsive force becomes dominant. A pH of higher than 7.5 was not examined because the magnetic nano-particles were dissolved in alkaline pH. The kinetic sorption of letrozole at pH 4 is presented in Fig. 4.

The sorption rate of letrozole was quite rapid, such that about 15 min shaking was required for 100% saturation sorption. The half time of saturation sorption is just 2 min. The rapid adsorption of the letrozole can be attributed to the accessibility of an active site in polymer which grafted onto the FPG-MNP. Scatchard analysis was carried out to evaluate the maximum sorption capacity. The Scatchard equation can be expressed as follows:

$$Q/C = (Q_{max} - Q)/K_d \quad (2)$$

where Q (μmol g^{-1}) is the equilibrium adsorption amount at each concentration; C (μmol mL^{-1}) is the equilibrium concentration of letrozole; Q_{max} (μmol g^{-1}) is the maximum adsorption of letrozole; and K_d (μmol mL^{-1}) is the equilibrium dissociation constant.

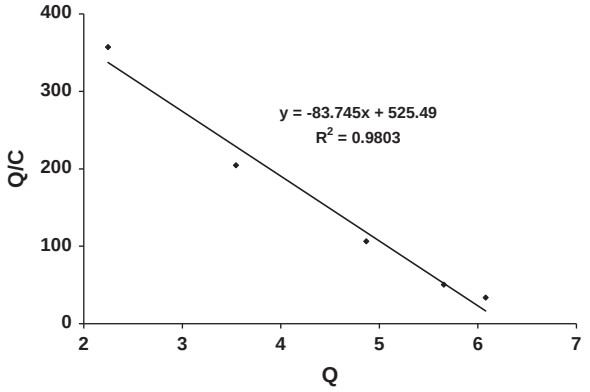

Fig. 5. Scatchard plots of letrozole adsorption onto FPG-MNP at 20 °C.

Table 2
Evaluation recovery in the different eluent.

Eluent	Recovery (%)
MeOH	76.4
MeOH/TFA (99:1)	81.4
MeOH/AcOH (98:1)	79.2
MeOH/TFA/AcOH (98.5:1/0.5)	77.3
MeOH/TFA/AcOH (98:1: 1)	97.8
MeOH/TFA/AcOH (94:1:5)	99.2

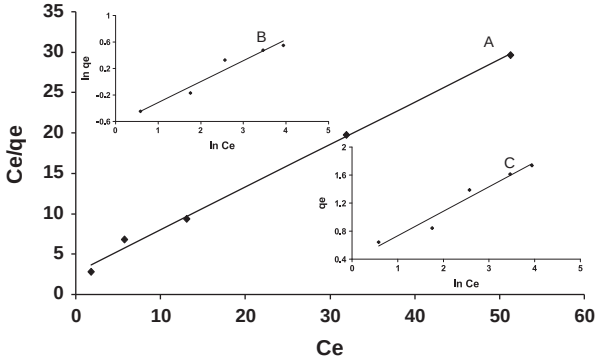

Fig. 6. Langmuir (A), Freundlich (B) and Temkin (C) isotherms for letrozole adsorption onto FPG-MNP at 20 °C.

The equation analysis shown in Fig. 5 indicates that K_d and Q_{max} were 0.012 μmol mL^{-1} and 6.27 μmol g^{-1}, respectively. The effects of various eluents on the extraction recovery of letrozole were also investigated. Eluents used were methanol and a small percentage of AcOH and TFA, added to improve the elution of drugs [26–28]. Obtained results, as from the HPLC analysis listed in Table 2, demonstrated that the methanol containing AcOH and TFA with a ratio of 94:1:5 (v/v) allows for the best removal of letrozole from FPG-MNP.

3.3. Adsorption isotherms

Adsorption isotherms are the presentation of the amount of letrozole adsorbed per unit of FPG-MNP. As a function of equilibrium concentration at 20 °C, the adsorption isotherms were evaluated for optimized letrozole removal (see Fig. 6). The Langmuir isotherm is valid for monolayer sorption on a surface with a number of identical active sites. This model assumes uniform energies of sorption on the modified surface and no transmigration of sorbate in the plane of the surface. The Langmuir equation

Table 3
Isotherm parameters obtained by using linear method at 20 °C.

Langmuir isotherm model			
q_{max} (mg g^{-1})	K_L (L mg^{-1})	R_L	R^2
1.90	0.19	0.08	0.9957
Frendlich isotherm model			
K_F (mg g^{-1}) (L $mg^{-1})^{1/n}$	n		R^2
0.53	3.16		0.9543
Temkin isotherm model			
A (L g^{-1})	B	b (J mol^{-1})	R^2
2.99	0.35	6969	0.9580
Redlich–Peterson isotherm model			
g	B (L $mg^{-1})^g$	A (L g^{-1})	R^2
0.92	0.47	0.6	0.9908

Table 4
Determination of letrozole in different samples.

Sample	Concentration of letrozole (μg mL^{-1})	Added (μg mL^{-1})	Found [a] (μg mL^{-1})	Recovery (%)
Plasma	–	2.00	1.63 ± 0.22	81.5
Urine	–	2.00	1.90 ± 0.12	95.0
Tablet	2.00	–	1.69 ± 0.30	84.5

[a] For three determinations.

is shown as [29]:

$$C_e/q_e = (1/q_{max}K_L) + (C_e/q_{max}) \quad (3)$$

where q_{max} is the maximum letrozole sorption capacity corresponding to complete monolayer coverage on the FPG-MNP surface (mg g^{-1}), and K_L is the Langmuir constant (L mg^{-1}). Langmuir parameters calculated from the Eq. (3) for letrozole sorption are listed in Table 3. The essential characteristics of the Langmuir equation can be expressed in terms of a dimensionless separation factor, R_L, defined as:

$$R_L = 1/(1 + K_L C_0) \quad (4)$$

The literature survey [30] revealed that the R_L value shows the adsorption nature to be either irreversible ($R_L = 0$), favorable ($0 < R_L < 1$), linear ($R_L = 1$), or unfavorable ($R_L > 1$). As seen in Table 3, the value of R_L (0.08) was in the range of 0–1, which confirms the favorable sorption of letrozole.

The Freundlich isotherm is an empirical isotherm employed to define heterogeneous systems in which it is determined by the heterogeneity factor $1/n$ with the empirical equation [31]:

$$\ln q_e = \ln K_F + 1/n \ln C_e \quad (5)$$

where K_F is the Freundlich constant (mg g^{-1}) (L $mg^{-1})^{1/n}$.

The empirical evidence of this model is based on adsorption on a heterogeneous modified surface. The Freundlich isotherm assumes a logarithmic decrease in the enthalpy of adsorption with an increase in the fraction of occupied active sites. The Freundlich isotherm predicts that the letrozole concentration on the FPG-MNP will increase as long as the letrozole concentration in the solution increases. Freundlich constants are listed in Table 3.

The Temkin equation suggests a linear decrease of sorption energy occurs as the degree of completion of the sorptional centers of FPG-MNP is increased [32]:

$$q_e = B \ln A + B \ln C_e \quad (6)$$

where $B = RT/b$ and b is the Temkin constant related to heat of letrozole sorption (J mol^{-1}). A is the Temkin isotherm constant (L g^{-1}), R (8.314 J mol^{-1} K^{-1}) is the gas constant, and T is the

Table 5
Analytical performance of letrozole determination.

	Analytical calibration curve	R^2	Linear range (μg mL^{-1})	RSD [a]		LOD (ng mL^{-1})	LOQ (ng mL^{-1})
				Repeatability	Reproducibility		
1	$Y=92X+0.072$	0.9629	0.2–100	0.97	1.08	13	43

[a] For four experiments.

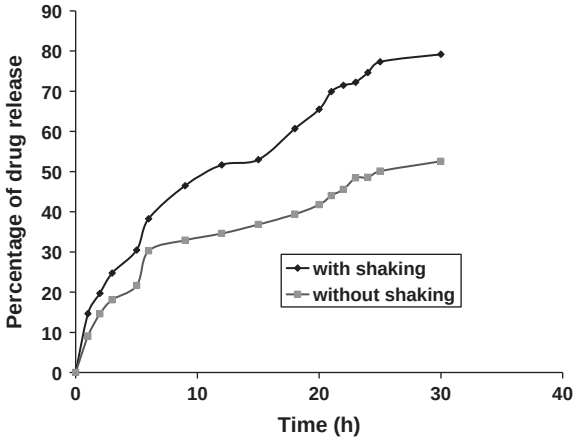

Fig. 7. Letrozole release profile in simulated intestinal fluid (pH 7.4).

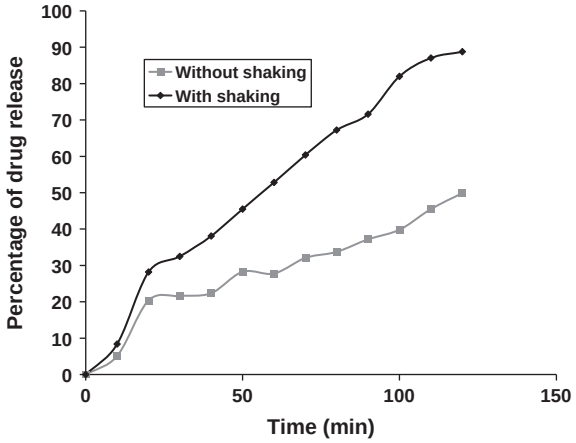

Fig. 8. Letrozole release profile in simulated gastric fluid (pH 1.2).

absolute temperature (K). Temkin isotherm constants are listed in Table 3.

The Redlich–Peterson isotherm has three constants, A, B, and g ($0<g<1$), and incorporates the features of the Langmuir and the Freundlich isotherms [33]:

$$\ln\left(A\frac{C_e}{q_e}-1\right)=g\ln(C_e)+\ln(B) \quad (7)$$

The Redlich–Peterson isotherm parameters for the sorption of letrozole onto FPG-MNP using linear regression are listed in Table 3. The results showed that the values of g were close to 1, which means that the isotherms are approaching the Langmuir form.

3.4. Method application

In order to study the suitability and applicability of the proposed method for the determination of letrozole in real samples, the developed solid phase extraction technique was applied for the extraction of this breast cancer inhibiting drug from human biological fluids and pharmaceutical samples. The extractions at optimum conditions were performed for human serum and urine as extractant samples without any pretreatments. The red blood cells were separated from human blood by centrifugation at 4600 × g for 20 min at room temperature, then filtered and frozen at −20 °C before use. Human blood was found to be negative for HCV (hepatitis C), HBS antigen and HIV I, II antibodies. The serums from human blood and human urine were spiked with letrozole before being subjected to the recommended procedure. To the best of our knowledge, there is strong competition for letrozole binding between serum components and active sites on the FPG-MNP. The results presented in Table 4 show a good recovery in human serum and urine indicating the power of FPG-MNP in letrozole extraction and also the reasonability and reliability of the presented method's procedure. Due to the importance of the analysis of letrozole in pharmaceutical samples, twenty tablets were extracted with methanol of HPLC grade, until a solid residue remained. Then, the proposed method was performed under optimized conditions. The results in Table 4 indicate the applicability of the procedure with reasonable recovery.

3.5. Analytical approach

The linearity and precision for letrozole in the developed method are presented in Table 5. The calibration curves were plotted using spiked standards at different letrozole concentrations under the optimized sorption condition. The limit of detection and limit of quantification corresponding to three and ten times the blank standard deviations are listed in Table 5. The repeatability and reproducibility of the method were the relative standard deviations (RSDs) for four replicate determinations of the sample at a 2 μg mL^{-1} level of letrozole in one day and on three different days (four times a day), respectively. Table 5 shows that the proposed method performed well analytically for FPG-MNP: the RSDs were less than 1.1%, and the R^2 value of the proposed method was over 0.95.

3.6. Letrozole release

The releasing of letrozole by FPG-MNP in simulated intestinal fluid (pH 7.4) was shown in Fig. 7, and in simulated gastric fluid (pH 1.2) was also indicated in Fig. 8. Approximately, 79% and 53% of the letrozole were released in the simulated intestinal fluid in with and without shaking mode over a period of 30 h at 37 °C; respectively. However, in the simulated gastric fluid (due to the harsh acetic media), letrozole was better released. Around 89% and 50% of letrozole can be released in about 120 min in with- and without-shaking modes at 37 °C, respectively.

4. Conclusions

Novel polymer grafted magnetic nano-particles were introduced for high letrozole extraction levels and then followed by HPLC determination. The results illustrate that the proposed technique has some advantages with respect to little solvent consumption, simplicity, high chemical stability and extraction efficiency. The sorption rate of the investigated letrozole on FPG-MNP was excellent. FPG-MNP combined with HPLC can be applied to the determination of trace letrozole in biological human fluids and pharmaceutical samples with satisfactory results.

Appendix A. Supplementary material

Supplementary data associated with this article can be found in the online version at http://dx.doi.org/10.1016/j.talanta.2013.09.015.

References

[1] A. Monnier, The Breast 15 (2006) S21–S29.
[2] M. Aydin, B. Yilmaz, E. Alcin, V.S. Nedzvetsky, Z. Sahin, M. Tuzcu, Neuroscience 151 (2008) 186–194.
[3] A. Awada, F. Cardoso, C. Fontaine, L. Dirix, J. de Greve, C. Sotiriou, J. Steinseifer, C. Wouters, C. Tanaka, U. Zoellner, P. Tang, M. Piccart, Eur. J. Cancer 44 (2008) 84–91.
[4] A.S. Bhatnagar, The Breast 15 (2006) S3–S13.
[5] X. Tao, H. Piao, D.J. Canney, M.R. Borenstein, I.P. Nnane, J. Pharm. Biomed. Anal. 43 (2007) 1078–1085.
[6] K.E. Kil, A. Biegon, Y.S. Ding, A. Fischer, R.A. Ferrieri, S.W. Kim, D. Pareto, M.J. Schueller, J.S. Fowler, Nucl. Med. Biol. 36 (2009) 215–223.
[7] I. Kijima, T. Itoh, S. Chen, J. Steroid Biochem. Mol. Biol. 97 (2005) 360–368.
[8] W.R. Miller, J.M. Dixon, L. Macfarlane, D. Cameron, T.J. Anderson, Eur. J. Cancer 39 (2003) 462–468.
[9] K. Gelmon, The Breast 16 (2007) 446–455.
[10] I.E. Smith, J. Steroid Biochem. Mol. Biol. 86 (2003) 289–295.
[11] Q. Gao, Q. Liang, F. Yub, J. Xu, Q. Zhao, B. Sun, Colloids Surf., B: Biointerfaces 88 (2011) 741–748.
[12] O. Veiseh, J.W. Gunn, M. Zhang, Adv. Drug Delivery Rev. 62 (2010) 284–304.
[13] C. Sun, J.S.H. Lee, M. Zhang, Adv. Drug Delivery Rev. 60 (2008) 1252–1265.
[14] H. Ai, Adv. Drug Delivery Rev. 63 (2011) 772–788.
[15] C.S.S.R. Kumar, F. Mohammad, Adv. Drug Delivery Rev. 63 (2011) 789–808.
[16] F. Rodriguez, Principals of Polymer Systems, 2nd ed., McGraw Hill, New York, 1982.
[17] A.E. Ivanov, J. Eccles, H. Ahmad Panahi, A. Kumar, M.V. Kuzimenkova, L. Nilsson, B. Bergenstahl, N. Long, G.J. Phillips, S.V. Mikhalovsky, I.Y. Galaev, B. Mattiasson, J. Biomed. Mater. Res. Part A 88 (2009) 213–217.
[18] M. Jahanshahi, H. Ahmad Panahi, S. Hajizadeh, E. Moniri, Chromatographia 68 (2008) 41–48.
[19] A.E. Ivanov, H. Ahmad Panahi, M.V. Kuzimenkova, L. Nilsson, B. Bergenstehl, S. Waqif Hosain, M. Jahanshahi, I.Y. Galaev, B. Mattiasson, Chem. Eur. J 12 (2006) 7204–7208.
[20] C. Zhang, L.Q. Zhao, Y.F. Dong, X.Y. Zhang, J. Lin, Z. Chen, Eur. J. Pharm. Biopharm. 76 (2010) 10–16.
[21] Y. Zu, Y. Zhang, X. Zhao, C. Shan, S. Zu, K. Wang, Y. Li, Y. Ge, J. Biol. Macromol. 50 (2012) 82–87.
[22] Y. Li, H. He, X. Jia, W.L. Lu, J. Lou, Y. Wei, Biomaterials 33 (2012) 3899–3908.
[23] P.P. Nampi, V.S. Mohan, A.K. Sinha, H. Varma, Mater. Res. Bull. 47 (2012) 1379–1384.
[24] A.R. Mahdavian, M.S. Mirrahimi, Chem. Eng. J 159 (2010) 264–271.
[25] H. Ahmad Panahi, J. Morshedian, N. Mehmandost, E. Moniri, I.Y. Galaev, J. Chromatogr. A 1217 (2010) 5165–5172.
[26] C. Baggiani, C. Giovannoli, L. Anfossi, C. Tozzi, J. Chromatogr. A 938 (2001) 35–44.
[27] G. Theodoridis, A. Kantifes, P. Manesiotis, N. Raikos, T.P. Heleni, J. Chromatogr. A 987 (2003) 103–109.
[28] E.P.C. Lai, S.G. Wu, Anal. Chim. Acta 481 (2003) 165–174.
[29] I. Langmuir, J. Am. Chem. Soc. 40 (1918) 1361–1368.
[30] K.L. Hall, L.C. Eagleton, A. Acrivos, T. Vermeulen, Ind. Eng. Chem. Fundam. 5 (1966) 212–218.
[31] H.M. Frendlich, J. Phys. Chem. 57 (1906) 385–390.
[32] M.I. Temkin, V. Pyzhev, Acta Physiochim. 12 (1940) 327–356.
[33] O. Redlich, D.L. Peterson, J. Phys. Chem. 63 (1959) 1024–1032.